ISSN 2829-4998

Performance optimization of a thermoelectric energy harvesting system utilizing waste heat from an internal combustion engine

Baribuma Gbaarabe [a,1,*], John I. Sodiki [a,2], Barinaadaa Thaddeus Lebele-Alawa [a,3], Barinyima Nkoi [a,4]

[a] Department of Mechanical Engineering , Rivers State University, P.M.B. 5080, Port Harcourt, Nigeria
[1] buma3g@gmail.com; [2] sodiki.john@ust.edu.ng; [3] lebele-alawa.thaddeus@ust.edu.ng; [4] nkoi.barinyima@ust.edu.ng
* corresponding author

ARTICLE INFO

Article history
Received July 25, 2025
Revised August 31, 2025
Accepted August 31, 2025
Available online September 26, 2025

Keywords
Design and performance optimization
Plate heat exchanger (PHE)
Thermoelectric module (TEM)
Thermoelectric energy harvesting (TEH) system
Waste heat from internal combustion engines (ICEs)

ABSTRACT

This study presents the performance optimization of a Thermoelectric Energy Harvesting (TEH) system designed to recover waste heat from Internal Combustion Engines (ICEs). It includes optimizing the energy conversion efficiency of the thermoelectric module (TEM), optimizing the design of the Plate Heat Exhcanger (PHE), and simulation-based validation. The optimization process, conducted using Python optimization code developed for the study, yielded an energy conversion efficiency of 7.209%, marking a 56% improvement over the experimentally measured efficiency of 4.63%. The optimized PHE design, incorporate finless triangular-rectangular composite duct. The analysis showed a fully turbulent flow within the PHE, which significantly enhances convective heat transfer coefficients, improve the heat exchange between the exhaust gas and heat exchanger surfaces, and reduces the risk of fouling and clogging. The exhaust gas contained 1792W of waste heat, with 230W transferred to the hot side of the TEM. This corresponds to a heat exchanger effectiveness of 0.13, indicating that only 13% of the available waste heat in the exhaust gas is utilized by the TEM. The overall TEH system efficiency was determined to be 0.94%, which, despite being relatively modest, yields considerable energy savings in large-scale applications where waste heat is abundant. Computational simulations, using a CAD model in SOLIDWORKS, validated the TEH system's optimized performance, by ensuring the desired temperature gradient is maintained across the TEM, given that the power output of the TEH is directly proportional to the temperature gradient across the thermoelectric couples in the TEM.

1. Introduction

The Internal Combustion Engines (ICEs) remains a vital component of the global energy infrastructure, widely used in transportation systems, industrial processes, and power generation. However, ICEs exhibit significant thermal inefficiencies, with approximately 20–50% of its input energy lost as waste heat, primarily in the form of exhaust gases discharged into the environment at temperatures exceeding 300°C [1], [2]. Waste heat recovery technologies offer the potential to utilize this waste heat, and reduce fossil fuel consumption, lowering greenhouse gas emissions, and improving the economic viability of power generation systems [1]. Among emerging waste heat recovery technologies, Thermoelectric Energy Harvesting (TEH) systems have gained attention for their ability to convert

https://doi.org/10.3176/aet.v4i2.2093

waste heat directly into electrical energy through the Seebeck effect. Seebeck effect is a phenomenon that occurs when a temperature gradient is applied across thermoelectric materials, typically composed of p-type and n-type semiconductors, causing charge carriers (electrons and holes) to diffuse from the hot side to the cold side, thereby generating a voltage difference [3].

The increasing adoption of TEH systems is driven by their solid-state operation, modularity, and scalability. Their modularity facilitates integration with existing infrastructure, while scalability supports a wide range of applications, from small Internet of Things (IoT) devices to large-scale industrial systems [4]. Despite these advantages, several limitations continue to impede their large-scale applications. These include the inherently low energy conversion efficiency of commercial TEMs (typically between 5% and 7%), significant thermal losses at the interfaces between the heat source and TEMs reduce the effective heat input, and challenges in maintaining a stable temperature gradient across the TEMs that is critical for consistent power generation. Collectively, these constraints limit the energy yield, scalability, and cost-effectiveness of TEH systems [5], [6].

While TEH systems offer a significant potential for waste heat recovery, overcoming existing limitations is essential to facilitate their large-scale application. To address these limitations, recent studies have focused on performance optimization through advancements in thermoelectric materials, adaptive thermal management strategies, innovative system design, and hybridization with complementary energy systems. Some of the recent studies are reviewed as follows: Reference [7] developed a TEG operating under constant heat flux using a simulation tool for geometrical optimization of the device. The simulation was performed by varying the number of pellets and the clearance between them. The results showed that high power was obtained with a large number of pellets, and enough clearance between the pellets, which was required to increase the thermal conductivity of the device.

Reference [8] carried out a simulation and experimental validation study on the transient behavior of a power generation system combining exhaust heat recovery device and TEM. The system was designed such that the exhaust heat recovery device would provide a source of heat to the TEM. A thermoelectric model was developed for the performance of waste heat recovery device. Also, a CFD analysis was performed to obtain the data of heat flux and temperature. The CFD model was coupled with the thermoelectric model to obtain the optimal power generating capacity of the system. Reference [9] investigated the optimization of a TEG-powered wireless sensor node designed for industrial applications. The system was experimentally tested using heat pipes of varying diameters to assess scalability. Results demonstrated successful energy harvesting from the temperature difference between the heat pipe and ambient air. Optimization analysis confirmed that the harvested power is sufficient for practical use in industrial wireless sensor node applications.

Reference [10] evaluated the performance of TEMs in recovering waste heat from LPG stoves, focusing on the impact of various cooling methods. Using four TEMs connected in series, they tested three cooling systems: a heatsink, a fan-assisted heatsink, and a water block. Results showed that heat absorption increased by over 300% with the fan-assisted heatsink compared to the standalone heatsink and by an additional 27% with water cooling. The water block system also yielded the highest power output, leading to the conclusion that water cooling optimize TEG performance in waste heat recovery applications. Reference [11] reviewed various ways to hybridize TEGs with renewable energy sources for optimal performance. They explored TEG integration with biomass systems for waste heat recovery from gasifiers, enhancing performance by optimizing surface contact and heat structures. In fuel cell systems, hybridizing with TEGs improved efficiency and thermal performance by regulating temperature and capturing additional waste heat. TEG integration with solar photovoltaics increased energy conversion efficiency, reduced overheating, and extended the lifespan of solar cells. The review concluded that TEGs could boost renewable energy system efficiency.

Reference [12] studied the hybridization of TEG and solar systems for air conditioning in an educational building. The TEG system that derived its source of heat from diesel engine's exhaust gasses complemented the energy generated by the solar system. The study concluded that the hybrid energy system provided an optimal solution for meeting the building's cooling load. Reference [13] explored waste heat recovery in autonomous aerial vehicles using a TEH system. The study achieved optimal performance through triangular plate-fin heat exchangers designed to efficiently capture thermal energy from engine exhaust streams. A longitudinal trapezoidal fin cylindrical heatsink was developed to amplify heat dissipation via forced convection, with its design refined through finite element analysis. This optimization maximized the thermal gradient across the integrated TEMs, resulted in increase in electrical output. The authors further developed a computational system model to simulate exhaust gas dynamics, enabling real-time performance. Experimental and numerical validation confirmed the system's feasibility, demonstrating stable power generation across flight cycles and reinforcing its potential for integration into next-generation autonomous aerial vehicles energy recovery systems.

Despite the potential of TEH system for waste heat recovery and optimal solutions to the limitations reported in the literatures, thermoelectric technology remains in a developmental phase and continues to face significant implementation challenges, necessitating further research for optimal and innovative design. For instance the triangular plate-fin heat exchanger employed by Reference [13] for optimal performance does not address uniform heat distributions that improve efficiency, as triangular fins can create higher flow resistance, leading to an increased pressure drop across the heat exchanger; which can reduce the flow rate of the exhaust gases and consequently affect the heat transfer performance. This present study employs a plate heat exchanger (PHE) configured with a hybrid duct design comprising both rectangular and triangular channels, to optimize heat transfer and exhaust gas flow dynamics. The study also utilizes advanced bismuth-telluride-based TEM doped with semiconductors from lead telluride to enhance their operating temperature range and electrical conductivity. The thermal performance optimization was further validated through simulations.

2. Method

The materials used in this study include the thermophysical property data of the exhaust emissions from the gasoline generator, design specifications of the TEM and the PHE, as well as Python and SOLIDWORKS simulation software.

2.1. Data Collection

The data used in this study comprise the properties of gasoline exhaust emissions, including temperature, density, thermal conductivity, specific heat capacity, and volumetric flow rate, obtained from established thermodynamic data tables. In addition, the design specifications and experimentally determined performance parameters of both the TEM and the PHE were obtained from Reference [14]. These data were used in the analysis and optimization processes. A summary of the key parameters is presented in Table 1.

Table 1. Design Specifications and Experimentally Determined Performance Parameters of TEH System Components

Components	Parameter	Value
Gasoline Generator: (RD3910EX) Model	Fuel	Gasoline
	Temperature of exhaust: At full load	400°C to 500°C
	Exhaust emission	7.33l/s (0.00733m³/s)
	Thermal conductivity of exhaust gas	0.054W/mK
	Density of exhaust gas	0.505kg/m³
	Specific capacity of exhaust gas	1152J/kgK
	Dynamic viscosity of exhaust gas	3.196×10^{-5}kg/ms
TEM: (1261G-7L31-04CQ) Model	Dimension of TEM	40mm×40mm×3.8mm
	Hot side temperature of TEM	320°C
	Cold side temperature of TEM	30°C
	Energy Conversion Efficiency	4.63%
	Thermal conductivity of TEM	1.2W/mK
	Material of TEM	Bismuth telluride(Bi_2Te_3)
PHE: (Finless Triangular-Rectangular Composite Duct)	Material of PHE	0.4mm stainless steel
	Thermal conductivity of PHE	16.5W/mK
	Dimension of rectangular duct of PHE	40mm×40mm×10mm
	Dimension of triangular duct of PHE	40mm×20mm×5mm

[a] Source: [14]

2.2. Optimization of the Prototype TEH System

Optimization is a systematic methodology for improving system performance by strategically adjusting operational parameters to achieve defined objectives, such as maximizing efficiency, minimizing costs, or enhancing reliability [15]. In this study, optimization was applied to maximize energy conversion efficiency of the TEH system.

2.2.1. Optimizing the Energy Conversion Efficiency of the TEM

This study employed a linear programming optimization method to maximize the energy conversion efficiency of the TEM. The optimization process was conducted under specific constraints, including the temperature gradient between the hot and cold sides (ΔT), the heat absorption rate (Q), and the power output of the TEM (P). To achieve optimal performance, the optimization problem was formulated based on the regression model developed by [14].

$$Maximize:\ \eta = 0.0002(\Delta T) + 0.0005(Q) + 0.002(P) - 0.0123$$

$$Subject\ to\ the\ constraints: \begin{cases} 60.70 \le \Delta T \le 160.4 \\ 31.08 \le Q \le 82.13 \\ 0.7 \le P \le 4.670 \end{cases} \quad (1)$$

2.2.2. Optimizing the Design of the PHE

Maximizing the thermal performance of the PHE requires optimization of key design parameters. These include designing the PHE geometry to enhance heat transfer efficiency by maximizing surface area and optimizing flow paths, selecting materials with high thermal conductivity and corrosion resistance to ensure long-term reliability under harsh operating conditions, and adopting a flow configuration that enhances turbulence, thereby increasing convective heat transfer rates. The optimized PHE designed incorporates a hybrid duct configuration featuring both rectangular and triangular cross-sectional geometries to enhance thermal performance and exhaust gas flow dynamics. The rectangular ducts ensure uniform thermal distribution and provide effective surface contact with the externally mounted TEM, thereby improving heat transfer performance. The triangular ducts feature a larger cross-sectional area at the inlet and a smaller one at the outlet, designed to streamline exhaust gas flow, minimizing flow resistance while inducing turbulence. This induced turbulence promotes both convective and conductive heat transfer; and ensuring more effective thermal energy exchange with the TEM. Fig. 1 shows the schematic of the optimized PHE design.

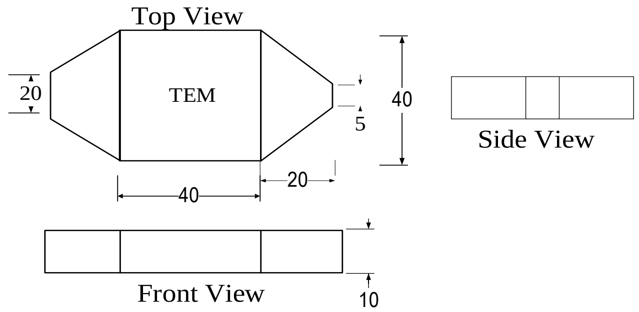

Fig. 1. Schematic of the Optimized PHE Design (Conceptualization)

Fig. 2 shows the 3-D model of the optimized PHE design.

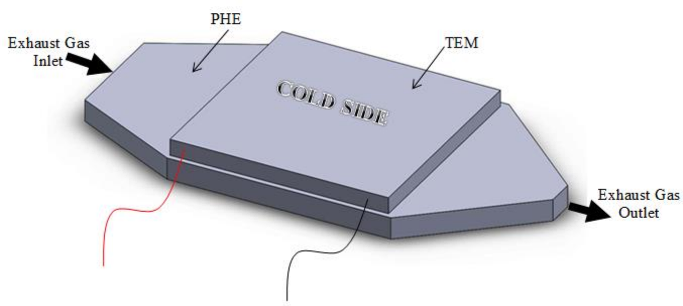

Fig. 2. 3-D model of the Optimized PHE Design (Conceptualization)

Also, a finless PHE configuration was chosen for the optimized design, as it is particularly well-suited for handling particle-laden fluids, such as exhaust gases. Unlike conventional fin-type PHEs, the finless design reduces the risk of fouling and clogging, thereby enhancing operational reliability and minimizing maintenance requirements. Collectively, these design optimizations make it more sustainable and efficient for waste heat recovery applications

2.3. Optimized PHE Performance Parameters

The performance parameters of the optimized PHE were assessed through exhaust gas flow and heat transfer analyses:

2.3.1. Exhaust Gas Flow

The exhaust gas flow was analyzed by evaluating its thermophysical properties and flow characteristics within the PHE. This analysis incorporated key dimensionless numbers and empirical correlations. The Reynolds number (Re) was used to characterize the flow regime and turbulence intensity, the Prandtl number (Pr) defined the relationship between momentum diffusivity and thermal diffusivity, and the Nusselt number (Nu) quantified the convective heat transfer coefficient.

- Reynolds Number

The Reynolds number (Re) of the exhaust gas was calculated using the following formula [16].

$$Re = \frac{\rho_{exh} \times u_{exh} \times d_{phe}}{\mu_{exh}} \quad (2)$$

where ρ_{exh}= density of the petrol exhaust gas, u_{exh}= exhaust gas exit velocity from the heat exchanger, d_{phe} = hydraulic diameter of the heat exchanger, μ_{exh} = dynamic viscosity of the petrol exhaust gas. The exhaust gas exit velocity from the heat exchanger and hydraulic diameter of the rectangular duct section of the heat exchanger are given, respectively by [17], [18].

$$u_{exh} = \frac{v_{exh}}{a_{phe}} \quad (3)$$

and

$$d_{phe} = \frac{2 \times w_{phe} \times b_{phe}}{w_{phe} + b_{phe}} \quad (4)$$

where $\dot{V}_{exh}$ = volumetric flow rate of the petrol exhaust gas, a_{phe} = exhaust gas flow exit area of the heat exchanger, w_{phe} = width of the rectangular duct section of heat exchanger, b_{phe} = height of the rectangular duct section of heat exchanger.

- Prandtl Number

The Prandtl number (Pr) of the petrol exhaust gas was calculated using the following formula [16].

$$Pr = \frac{C_{Pexh} \times \mu_{exh}}{K_{exh}} \quad (5)$$

where CPexh = specific heat capacity of the petrol exhaust gas, k_{exh} = thermal conductivity of the petrol exhaust gas.

- Nusselt Number

The Nusselt number (Nu) was calculated using the Dittus-Boelter equation, a widely recognized empirical correlation in heat transfer engineering for estimating convective heat transfer in forced convection through non-circular ducts, where the hydraulic diameter serves as the characteristic length. This equation is specifically applicable to turbulent flow conditions, characterized by Reynolds numbers (Re > 4000), and Prandtl numbers (Pr) within the range 0.7 ≤ Pr ≤ 160. For heating processes, Dittus-Boelter equation is expressed as follows [16].

$$N_{u_{exh}} = 0.023 \times Re^{0.8} \times Pr^{0.4} \quad (6)$$

- Convective Heat Transfer Coefficient

The convective heat transfer coefficient (h_{exh}) of the exhaust gas was calculated using the following formula [16]:

$$h_{exh} = \frac{N_{u_{exh}} \times k_{exh}}{d_{phe}} \quad (7)$$

2.3.2. Heat Transfer Analysis

The schematic diagram of Fig. 3 illustrates the heat transfer in the prototype TEH system.

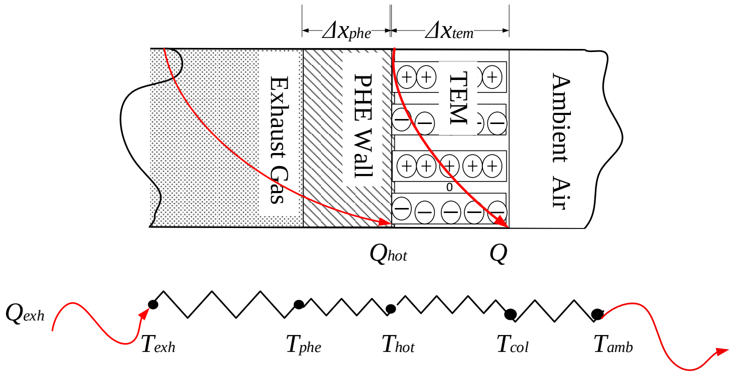

Fig. 3. Schematic Heat Transfer of the Prototype TEH System (Conceptualization)

- Heat Transfer Rate to the Hot Side of the TEM

The heat transfer rate to the hot side of the TEM (Q_{hot}) represents the amount of heat transferred from the exhaust gas, through the wall of the heat exchanger, to the hot side of the TEM. As shown in Fig. 3, it was calculated using the following equation [19].

$$Q_{hot} = \frac{T_{exh} - T_{hot}}{\frac{1}{h_{exh}A_{phe}} + \frac{\Delta x_{phe}}{k_{phe}A_{phe}}} \tag{8}$$

where T_{exh} = temperature of the exhaust gas, A_{phe} = area of the PHE covered by the TEM, Δx_{phe} = thickness of the PHE wall, k_{phe}= thermal conductivity of the PHE material.

- Available Waste Heat in the Exhaust Gas

The available waste heat in the exhaust gas (QQ_{exh}) was calculated using the equation [20].

$$Q_{exh} = v_{exh} \times \rho_{exh} \times C_{Pexh} \times (T_{exh} - T_{amb}) \tag{9}$$

- Effectiveness of the PHE

The effectiveness of a PHE is defined as the ratio of the actual heat transferred to the maximum possible heat transfer under identical operating conditions. It serves as a performance indicator in the design and evaluation of heat exchanger systems, with higher effectiveness indicating efficient performance. In this study, the effectiveness of the PHE represents the fraction of thermal energy transferred to the hot side of the TEM. Its value dependents on design parameters, including exhaust gas flow characteristics and the geometric configuration of the PHE. Thus, the effectiveness of the PHE was calculated given by the formula [21]:

$$\varepsilon_{phe} = \frac{Q_{hot}}{Q_{exh}} \tag{10}$$

2.3.3. Optimal Overall Energy Conversion Efficiency of the TEH System

The overall energy conversion efficiency measures the performance of the entire TEH system. It encompasses the energy conversion efficiency of the TEM in converting thermal energy into electrical energy (η_{teg}), and the effectiveness of the PHE in transferring heat to the TEM (ε_{phe}). The overall energy conversion efficiency ($\eta_{Overall}$) of the TEH system is given by [22].

$$\eta_{Overall} = \eta_{tem} \times \varepsilon_{phe} \tag{11}$$

2.4. Simulation of the TEH System

Fig. 4 illustrates the Computer-Aided Design (CAD) model of the TEM, depicting the arrangement of the thermoelectric couples.

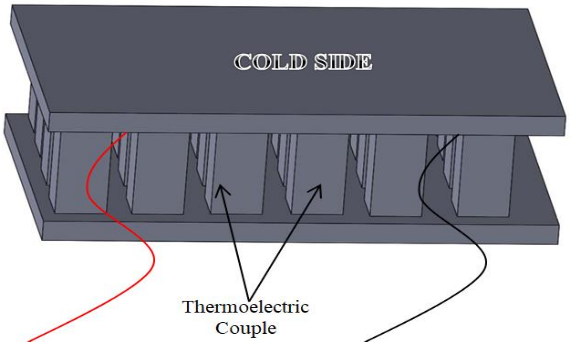

Fig. 4. CAD Model of the TEM

The optimized performance of the TEM was validated using a SOLIDWORKS-developed CAD model, with simulations quantifying the thermal gradient distribution across the module.

3. Results and Discussion

The results of the study are presented and discussed as follows.

3.1. Optimization Results

The objective of the optimization was to maximize the energy conversion efficiency (η) of the prototype TEH system, as defined by (1). Using a Python optimization code, the study achieved an optimal energy conversion efficiency of 7.209%, at a temperature difference of 160.4K, a heat absorption rate of 82.13W, and a power output of 4.67W. The optimized efficiency aligns closely with the record-high efficiency of approximately 7.3% reported by Reference [23], for an Mg_3Sb_2/MgAgSb-based TEM.

3.2. Optimal Convective Heat Transfer Coefficient

The optimal convective heat transfer coefficient for the exhaust gas flowing through the optimally designed PHE was determined as follows:

- Analysis of the Exhaust Gas Exit Velocity from the PHE

  The exhaust gas exit velocity from the PHE was determined using (3), considering that v_{exh} = 73.3L/s = 0.00733m^3/s, a_{phe}= 0.005 × 0.005 = 0.000025m^2 (from Fig. 1) .

$$u_{exh} = \frac{0.00733}{0.000025} \approx 293.2m/s$$

- Analysis of the Hydraulic Diameter of the PHE

  Using (4), the hydraulic diameter (d_{phe}) of the PHE was determined based on the given duct dimensions: w_{phe} = 0.04m, b_{phe} = 0.01 (from Table 1),

$$d_{phe} = \frac{2\times0.04\times0.01}{0.04+0.01} \approx 0.016m$$

- Analysis of the Reynolds Number of the Exhaust Gas

  The Reynolds number of the exhaust gas is determined using (2), noting that: u_{xeh} = 293.2m/s,

d_{phe} = 0.016m, ρ_{exh}= 0.505kg/m3, μ_{exh} = 3.196×10-5kg/ms (from Table 1)

$$Re = \frac{0.505\times 293.2\times 0.016}{3.196\times 10^{-5}} \approx 74.126$$

Since Re ≫ 4000, the analysis confirms a fully turbulent flow regime within the PHE. Turbulent flow is characterized by chaotic fluid motion and intense mixing, which significantly enhances convective heat transfer coefficients, and improve gas-to-surface thermal exchange [24].

- Analysis of the Prandtl Number of the Exhaust Gas

The Prandtl number of the exhaust gas is calculated using (5) as follows: C_{Pexh} = 1152J/kgK, μ_{exh} = 3.196×105 kg/ms, k_{exh}= 0.054W/mK (Table 1).

$$Pr = \frac{1152\times 3.196\times 10^{-5}}{0.054} \approx 0.7$$

The analysis yielded a relatively low Prandtl number (Pr < 1), which indicates rapid heat transfer due to high thermal diffusivity [25].

- Analysis of the Nusselt Number of the Exhaust Gas

Applying (6), the Nusselt number of the exhaust gas is determined as follows: Re = 74,126, Pr = 0.7

$$Nu_{exh} = 0.023 \times 74126^{0.8} \times 0.7^{0.4} \equiv 157$$

Thus, Using (7), the convective heat transfer coefficient of the exhaust gas is calculated thus: Nu_{exh} = 157, k_{exh} = 0.054 *W/mK* (from Table 1), d_{phe} = 0.016m

$$h_{exh} = \frac{157\times 0.054}{0.016} \approx 530W/m^2K$$

A convective heat transfer coefficient of 530 W/m²K is considered relatively high, indicating strong convective activity within the exhaust gas flow. Such a high value is typically associated with high gas velocity, turbulent flow conditions, and potentially optimized surface geometries that enhance thermal interaction. This value is within the expected range for turbulent exhaust flow in the PHE, where efficient heat transfer is essential for maximizing system performance

3.3. Equations

The equations are an exception to the prescribed specifications of this template. You will need to determine whether or not your equation should be typed using either the Times New Roman or the Symbol font (please no other font). To create multileveled equations, it may be necessary to treat the equation as a graphic and insert it into the text after your paper is styled.

3.4. Analysis of the Heat Transfer Rate to the TEM

The heat transfer rate from the exhaust gas to the TEM was determined using (8) as follows: T_{exh} = 723K, T_{hot} = 448.1K (from Table 1), h_{exh} = 524W/m2K, A_{phe} = 0.04 ×0.04 = 0.0016m2, Δ_{xphe} = 0.0004m, k_{phe} = 50W/mK (Table 1).

$$\dot{Q}_{hot} = \frac{723 - 448.1}{\dfrac{1}{524\times 0.0016} + \dfrac{0.0004}{50\times 0.0016}} \approx 230W$$

3.5. Analysis of the of the PHE Effectiveness

Using (10), we obtain the effectivenes of the PHE: $\dot{Q}_{hot}$ = 230W, $\dot{Q}_{exh}$ = 1792W

$$\varepsilon_{phe} = \frac{230}{1792} \approx 0.13$$

This result indicates that 13% of the total waste heat available in the exhaust gas was absorbed and transferred to the TEM.

3.6. Analysis of the Optimal Overall Energy Conversion Efficiency of the TEH System

Applying (11) we obtain the optimal overall energy efficiency of the TEH System thus: ε_{phe} = 0.13, η_{teg} = 0.07209.

$$\eta_{overall} = 0.07209 \times 0.13 \approx 0.0094$$

The overall energy efficiency of the TEH system was determined to be 0.0094, indicating that only 0.94% of the absorbed waste heat was converted into electrical energy. Although modest, such overall energy efficiency can yield considerable energy savings in large-scale applications where waste heat is abundant.

3.7. System Thermal simulation Result

Fig. 5 and Fig. 6 are the simulation results that depict the thermal performance of a TEH system. Fig. 5 shows the temperature distribution across the entire TEH system. The color scale to the left shows temperature values ranging from about 303K (blue) to 720 K (red). The red area represents the hot side, where the waste heat from the exhaust gases is applied. The blue area represents the cold side, cooled by ambient. The red-yellow transition areas show how heat is transferred from the exhaust gas inlet to the exhaust gas outlet. The red-green-blue transition areas show how heat is transferred from the hot side to the cold side.This figure gives an overall view of how temperature is distributed through the TEH structure.

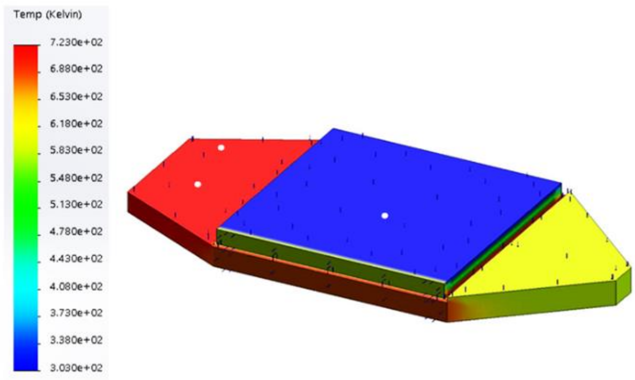

Fig. 5. Temperature Distribution across the entire TEH System

Fig. 6 provides a more detailed cross-sectional view of the temperature gradient across TEM. The temperature scale appears similar, with hot regions at the bottom (red) and cold regions at the top (blue). The vertical heat flow is clearly shown from the hot base, through the thermoelectric couples, up to the cooled top plate. The gradient is essential for thermoelectric power generation, as voltage is produced across the TEM when there is a significant temperature difference. This diagram focuses on how well each thermoelectric couple is performing in terms of maintaining a thermal gradient, which directly affects power output. These figures validated the optimized design of the TEH system by ensuring the desired temperature gradient is maintained across the TEM, given that the power output of the TEH is directly proportional to the temperature gradient across the thermoelectric couples in the TEM.

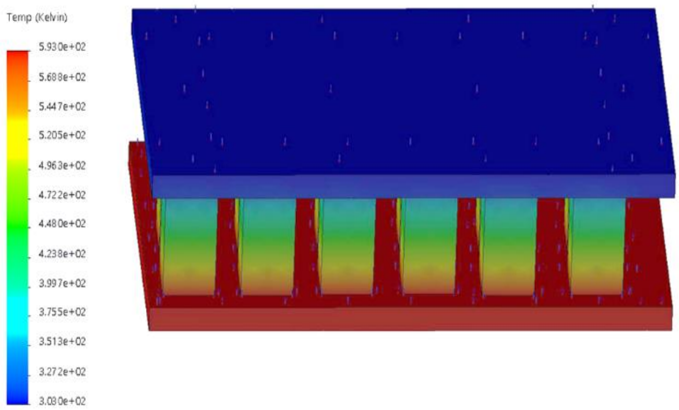

Fig. 6. Temperature Gradient across the TEM

4. Conclusion

This study presents the performance optimization of a TEH system, designed to recover waste heat from ICEs and convert it into usable electrical energy. The key findings are summarized as follows: 1) The optimization process, conducted using Python optimization code developed for the study, yielded an energy conversion efficiency of 7.209%, marking a 56% improvement over the experimentally measured efficiency of 4.63%; 2) The optimized PHE design, incorporates a finless triangular-rectangular composite duct. The analysis showed a fully turbulent flow within the PHE, which significantly enhances convective heat transfer coefficients, improving the heat exchange between the exhaust gas and the heat exchanger surfaces, and reduces the risk of fouling and clogging; 3) The exhaust gas contained 1792W of waste heat, with 230W transferred to the hot side of the TEM. This corresponds to a heat exchanger effectiveness of 0.13(13%), meaning only 13% of the available waste heat in the exhaust gas is utilized by the TEM; 4) The overall TEH system efficiency was determined to be 0.94%, which, despite being relatively modest yield considerable energy savings in large-scale applications where waste heat is abundant; 5) Computational simulations, using a CAD model in SOLIDWORKS, validated the TEH system's optimized performance, by ensuring the desired temperature gradient is maintained across the TEM, given that the power output of the TEH is directly proportional to the temperature gradient across the thermoelectric couples in the TEM. In conclusion, this study demonstrates the potential of TEH systems to effectively recover and convert thermal energy from ICE exhaust gases into usable electrical energy. The results highlight the importance of optimizing thermal and electrical parameters to maximize system performance. It is recommended that stakeholders in the energy sector implement supportive policies and incentives to accelerate the adoption of TEH systems in next-generation ICEs, aligning with global objectives for improved energy efficiency and reduced carbon emissions in industrial processes, transportation and power generation systems.

Acknowledgment

The authors wish to acknowledge the staff and students of Harvoxx Tech Hub, PortHarcourt, Nigeria for their assistance in developing the Python code used for the optimization of the energy conversion efficiency of the TEM.

Declarations

Author contribution. Baribuma Gbaarabe conceived the study, designed the optimal system, conducted simulations, and performed data collection and analysis. John I. Sodiki contributed to the editing of the manuscript. Barinaada Thaddeus Lebele-Alawa, and Barinyima Nkoi reviewed and approved the final version of the manuscript.

Funding statement. The authors received no financial support for the research, authorship, and/or publication of this article.

Conflict of interest. The authors declare no conflict of interest.

Additional information. No additional information is available for this paper.

References

[1] I. Johnson, W. Choate, and A. Davidson, "Waste Heat Recovery. Technology and Opportunities in U.S. Industry," Mar. 2008. doi: 10.2172/1218716.

[2] C. Forman, I. K. Muritala, R. Pardemann, and B. Meyer, "Estimating the global waste heat potential," *Renew. Sustain. Energy Rev.*, vol. 57, pp. 1568–1579, May 2016, doi: 10.1016/j.rser.2015.12.192.

[3] D. M. Rowe, *Thermoelectrics Handbook*. CRC Press, 2018, doi: 10.1201/9781420038903.

[4] P. Christodoulides, R. Agathokleous, L. Aresti, S. A. Kalogirou, S. A. Tassou, and G. A. Florides, "Waste Heat Recovery Technologies Revisited with Emphasis on New Solutions, Including Heat Pipes, and Case Studies," *Energies*, vol. 15, no. 1, p. 384, Jan. 2022, doi: 10.3390/en15010384.

[5] S. Davis, "Power Management Series," *Electronic Design*, 2022. [Online]. https://www.electronicdesign.com/technologies/power/article/21212387/electronic-design-power-management-series.

[6] K.-T. Lee *et al.*, "An overview of commercialization and marketization of thermoelectric generators for low-temperature waste heat recovery," *iScience*, vol. 26, no. 10, p. 107874, Oct. 2023, doi: 10.1016/j.isci.2023.107874.

[7] A. Montecucco, J. Siviter, and A. R. Knox, "Constant heat characterisation and geometrical optimisation of thermoelectric generators," *Appl. Energy*, vol. 149, pp. 248–258, Jul. 2015, doi: 10.1016/j.apenergy.2015.03.120.

[8] D. Champier, "Thermoelectric generators: A review of applications," *Energy Convers. Manag.*, vol. 140, pp. 167–181, May 2017, doi: 10.1016/j.enconman.2017.02.070.

[9] Y. J. Kim *et al.*, "High-performance self-powered wireless sensor node driven by a flexible thermoelectric generator," *Energy*, vol. 162, pp. 526–533, Nov. 2018, doi: 10.1016/j.energy.2018.08.064.

[10] N. T. Atmoko, T. W. B. Riyadi, B. R. Utomo, A. Jamaldi, and A. S. Nugroho, "Heat Transfer Analysis and Performance Investigation of Generator Thermoelectric Applied in LPG Stove Waste Heat Recovery," *Int. J. Renew. Energy Res.*, vol. 13, no. V13i1, pp. 70–76, Mar. 2023, doi: 10.20508/ijrer.v13i1.13137.g8696.

[11] Z. Wehbi, R. Taher, J. Faraj, C. Castelain, and M. Khaled, "Hybrid thermoelectric generators-renewable energy systems: A short review on recent developments," *Energy Reports*, vol. 8, pp. 1361–1370, Nov. 2022, doi: 10.1016/j.egyr.2022.08.068.

[12] Baribuma Gbaarabe and John I. Sodiki, "Hybridization of energy systems for air conditioning application in an educational building," *Glob. J. Eng. Technol. Adv.*, vol. 16, no. 2, pp. 092–105, Aug. 2023, doi: 10.30574/gjeta.2023.16.2.0137.

[13] R. B. Smriti *et al.*, "Thermoelectric Energy Harvesting for Exhaust Waste Heat Recovery: A System Design," *ACS Appl. Mater. Interfaces*, vol. 17, no. 3, pp. 4904–4912, Jan. 2025, doi: 10.1021/acsami.4c18023.

[14] B. Gbaarabe, "Development of a Large-Scale Thermoelectric Energy Harvesting System Utilizing Waste Heat from Thermal Power Plants," Univ., Port Harcourt, Nigeria, 2025.

[15] M. Groten and S. Gallego-García, "A Systematic Improvement Model to Optimize Production Systems within Industry 4.0 Environments: A Simulation Case Study," *Appl. Sci.*, vol. 11, no. 23, p. 11112, Nov. 2021, doi: 10.3390/app112311112.

[16] G. . Rogers and Y. Mayhew, *Engineering thermodynamics : work and heat transfer*. Pearson India Education Services, 2006. [Online]. Available at: https://dokumen.pub/engineering-thermodynamics-work-and-heat-transfer-4nbsped-8131702065-9788131702062.html.

[17] H. G. Zhang *et al.*, "Performance Analysis And Experimental Investigation On Exhaust Gas Heat Recovery For IC Engines Using Shell And Tube Heat Exchanger," *Int. J. Eng. Appl. Sci.*, vol. 4, no. 7, p. 257415, 2017. [Online]. Available at: https://www.neliti.com/publications/257415/.

[18] F. M. White and H. Xue, *Fluid Mechanics Textbook*, Ninth Edit. 2021. [Online]. Available at: https://studylib.net/doc/26335616/white-xue-fluid-mechanics-9th-edition.

[19] H. Jouhara *et al.*, "Thermoelectric generator (TEG) technologies and applications," *Int. J. Thermofluids*, vol. 9, p. 100063, Feb. 2021, doi: 10.1016/j.ijft.2021.100063.

[20] M. Bukowska, K. Nowak, D. Proszak-Miąsik, and S. Rabczak, "Concept of Heat Recovery from Exhaust Gases," *IOP Conf. Ser. Mater. Sci. Eng.*, vol. 245, no. 5, p. 052057, Oct. 2017, doi: 10.1088/1757-899X/245/5/052057.

[21] X. Qian, S. W. Lee, and Y. Yang, "Heat Transfer Coefficient Estimation and Performance Evaluation of Shell and Tube Heat Exchanger Using Flue Gas," *Processes*, vol. 9, no. 6, p. 939, May 2021, doi: 10.3390/pr9060939.

[22] B. Ryu *et al.*, "Best thermoelectric efficiency of ever-explored materials," *iScience*, vol. 26, no. 4, p. 106494, Apr. 2023, doi: 10.1016/j.isci.2023.106494.

[23] Z. Liu *et al.*, "Demonstration of ultrahigh thermoelectric efficiency of ~7.3% in Mg3Sb2/MgAgSb module for low-temperature energy harvesting," *Joule*, vol. 5, no. 5, pp. 1196–1208, May 2021, doi: 10.1016/j.joule.2021.03.017.

[24] W. M. . Kays, M. E. . Crawford, and B. Weigand, *Convective heat and mass transfer*. McGraw-Hill Higher Education, 2005.

[25] M. Mobedi and G. Gediz Ilis, *Fundamentals of Heat Transfer*. 2023, doi: 10.1007/978-981-99-0957-5.